Numerical Simulation and Experimental Study on Jet Forming and Penetration Performance of Zr-based Amorphous Alloy Liner

Ping Cui, Dongmei Shi, Yuling Zhang, and Deshi Wang

***Abstract*—It is an important trend for the development of shaped charge (SC) technology to use energetic material in liner. As a new metastable energetic material, zirconium (Zr) based amorphous alloy has incomparable advantages over other energetic materials. In order to understand the jet forming law of Zr-based amorphous alloy liner and acquire an accurate understanding of the influence of key factors such as cone angle and wall thickness on the jet parameters of this kind of liner, the conical ZrCuNiAlAg amorphous alloy liner is taken as a research object and some numerical simulation of the jet forming process are carried out including 5 cone angles under certain wall thickness conditions and 5 kinds of wall thicknesses under certain cone angle conditions based on AUTODYN software. The static explosion tests of Zr-based amorphous alloy liner against steel target plate are carried out as well. The results show that the conical ZrCuNiAlAg amorphous alloy liner can form a stable and continuous jet with a spindle shape under the action of explosive products. In a certain range, both the tip velocity and length diameter ratio (LDR) of the jet decrease with the increasing cone angle and wall thickness of the liner. The average penetration depth of a conical ZrCuNiAlAg amorphous alloy liner with 40° cone angle and 1.2mm wall thickness against 45# steel target plate is 97.5mm at the stand-off distance of 3 times of charge diameter (CD). The diameter of perforation entrance is 25mm. The deflagration reaction and the deflagration products' reverse flight and strong erosion through the orifice are the main reasons for the formation of "large diameter, small penetration depth" perforation by the jet, which shows obvious energy-releasing characteristics in the process of penetration. The above results have certain guiding significance for the structural design of Zr-based amorphous alloy liner and the SC.**

***Index Terms*—Shaped charge, Zr-based amorphous alloy, jet forming, liner, wall thickness, cone angle**

Manuscript received May 13, 2020; revised September 6, 2020. This work is supported by "Foundation Strengthening Project of Science and Technology Commission of Central Military Commission, PRC (No. 2017-JCJQ-ZD-022-03)" and the "Weapon Equipment Advance Research Project (No. 170441422086)".

Ping Cui is currently pursuing the PH.D. degree in Naval University of Engineering, Wuhan, Hubei, 430033, China and he is with Army Engineering University of PLA, No. 97 Heping West Road, Shijiazhuang, Hebei, 050003, China (e-mail: cctv2004re@163.com).

Dongmei Shi is with Army Engineering University of PLA, No. 97 Heping West Road, Shijiazhuang, Hebei, 050003, China(e-mail: 13383013059@163.com).

Yuling Zhang is with Army Engineering University of PLA, No. 97 Heping West Road, Shijiazhuang, Hebei, 050003, China (corresponding author to provide phone: +86031187994311; e-mail: pingjing1981@163.com).

Deshi Wang is with Naval University of Engineering, No. 717 Jiefang Street, Wuhan, Hubei, 430033, China (e-mail:wdeshi@sina.com).

Ⅰ. INTRODUCTION

Liners are the most vital components of shaped charge (SC), the material selection and structure design of which have significant influence on jet forming and damage performance of SC.

For a long time, the damage pattern of inert material metal jet to the target is usually "deep but small" holes. This single penetrating damage mode of "hitting without destroying" cannot meet the new requirements of modern war for efficient and comprehensive damage to the target. At present, the focus of scholars is to replace the traditional non-energetic inert materials with energetic materials in the field of SC. The application of new energetic materials on the SC makes it not only keep the high-efficient penetration effect, but also have the aftereffect of combustion, detonation and heat release, which further enriches the damage mode of the SC to the target. Some scholars have carried out in-depth research on the mechanical properties of PTFE/Al energetic materials and its damage mechanism of penetration and explosion[1-5]. The density of this type of energetic materials is relatively small, although the aftereffect is obvious, but its penetration depth is limited.

As a new type of energetic material, Zr-based amorphous alloy has high strength, high hardness and good energy release characteristics. The SC jet formed by this kind of metastable state material can produce violent chemical reaction during or after penetrating the target plate, release a lot of chemical energy, and eventually achieve much higher efficient damage. Walters[6-7] et al. from the US Army Research Laboratory studied the jet forming and penetration behavior of Zr-based amorphous alloy liner with the atomic composition of $Zr_{57}Nb_5Cu_{15.4}Ni_{12.6}Al_{10}$. The results show that Zr-based amorphous alloy liner has good jet forming and penetration ability. However, Walters only conducted a small number of static explosion tests due to the huge costs including 3 rounds of SC, two of which are free flight and the other one is penetration against steel target. He did not conduct further research on the influence of geometric parameters of liner on the forming performance of energetic jet. Han[8-9] et al. studied the application of tungsten/zirconium amorphous alloy composite liner with "a spherical segment and a frustum", but did not pay attention to the influence of liner parameters on jet performance.

The commonly used geometrical shapes of liners are conical, spherical and trumpet. The different shapes of liners have important influence on the jet morphology, velocity gradient and the maximum stretch length. Once the liner's shape is determined, the geometric parameters will have an important impact on the jet morphology and damage effect. Taking the most widely used conical SC as an example, the

cone angle and wall thickness are the two most important structural parameters, which are also the most two concerned parameters in the process of numerical simulation and experimental research of various SC by scholars. Manfred held[10] studied the influence of the liner's cone angle on the jet shape and velocity by means of the flash X-ray technology. The jet with a small cone angle has a long and thin head and a large tip velocity, while the one with a large cone angle has a short and thick head and a small tip velocity. In reference [11], the applicable cone angle ranges of metal jet (JET), rod penetration body (JPC) and explosive forged projectile (EFP) are given in detail by simulation. The results of some references[10], [12-14] on the influence of wall thickness show that the wall thickness can significantly affect the velocity distribution along the length direction of the jet, and the jet velocity increases with the decrease of wall thickness. However, this does not mean that the smaller the wall thickness, the better. On the one hand, too thin wall thickness cannot form normal jet; on the other hand, the operational use of warhead determines the jet-forming category of the liner and the specific jet-forming category requires that the wall thickness should meet certain conditions.

Based on a new type of Zr-based amorphous alloy energetic material, this paper studies the influence of cone angle and wall thickness on the jet forming and target-penetrating performance by means of numerical simulation and static explosion test, so as to accurately grasp the basic rules of the structure design for this kind of conical SC liner.

Ⅱ. MODEL OF SIMULATION

The SC is composed of explosive and liner, as shown in Fig. 1. The charge length is 100mm and the diameter is 40mm. C-4 explosive with density of 1.60g/cm^3 is used for charging and JWL equation of state is used to describe the expansion process of explosive detonation products. ZrCuNiAlAg five element amorphous alloy is used for the liner material, and JH-2 model[15] is used to describe its deformation and damage process. The JH-2 material parameters are listed in TableⅠ.

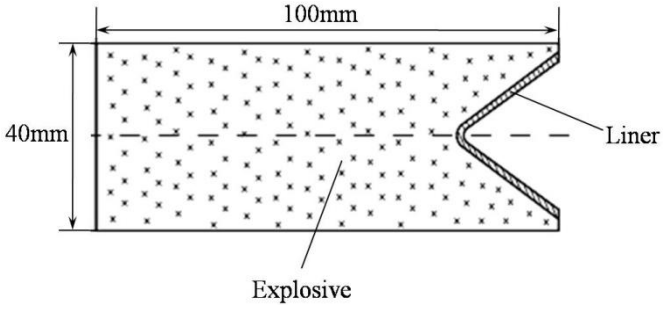

Fig.1. The structure of SC with a conical liner.

The air domain of 370mm×40mm is established by using the finite element simulation software of AUTODYN. Point initiation is adopted for SC. In order to eliminate the boundary effect, the calculation boundary condition is set as "flow_out (all equal)", so that the air and explosive gas can flow out normally when they reach the calculation boundary condition. Because the jet forming process is a high strain and high strain rate process, the Euler grid is used to calculate. In order to reduce the calculation amount, a two-dimensional axisymmetric calculation model is used in the whole simulation process. The established finite element model of numerical simulation is shown in Fig. 2.

TABLE Ⅰ THE JH-2 MATERIAL MODEL PARAMETERS OF ZrCuNiAlAg AMORPHOUS ALLOY

Parameter	Value
ρ/(g/cm^3)	6.581
A_1/(kPa)	1.117×10^8
A_3/(kPa)	8.044×10^9
G/kPa	3.704×10^6
B	0.258
M	0.59
D_1	0.005
σ_{HEL}(kPa)	3.467×10^6
A_2/(kPa)	4.037×10^8
T_1/(kPa)	1.117×10^8
A	1.397
C	0.0044
N	2.432
D_2	1

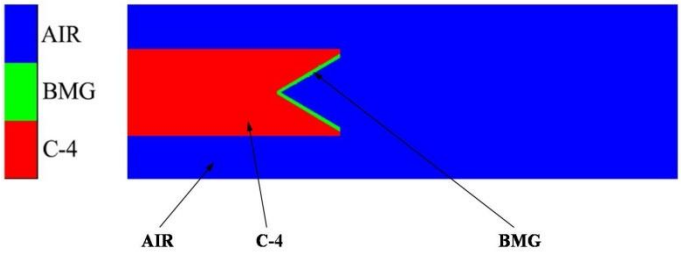

Fig.2. The finite element model.

Ⅲ. ANALYSIS OF NUMERICAL SIMULATION RESULTS

The jet morphology of ZrCuNiAlAg amorphous alloy conical liner from numerical simulation and the velocity distribution of the jet are shown in Fig. 3. It can be seen from the figure that the jet is overall spindle shaped, with good forming performance and flight stability. When the jet reaches 170mm, the tip velocity is about 4390m/s.

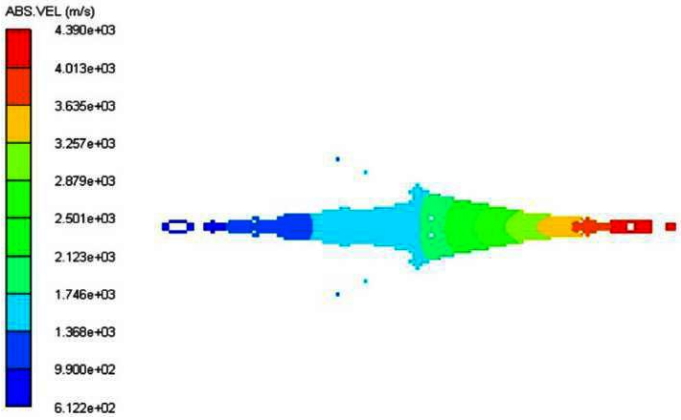

Fig.3. The velocity distribution cloud map of ZrCuNiAlAg jet.

The cone angle and the wall thickness of the conical liner

are changed respectively while other parameters of the shaped charge remain unchanged. The influence of the liner parameters on the jet forming of ZrCuNiAlAg amorphous alloy is obtained by simulation.

A. Influence of cone angle on jet forming performance

Based on the structure of SC shown in Fig. 1, the wall thickness of the SC is set to 0.8mm. The jet forming process of ZrCuNiAlAg amorphous alloy is simulated when the cone angle is 40 °, 60 °, 80 °, 100 ° and 120 ° respectively, as shown in Fig. 4.

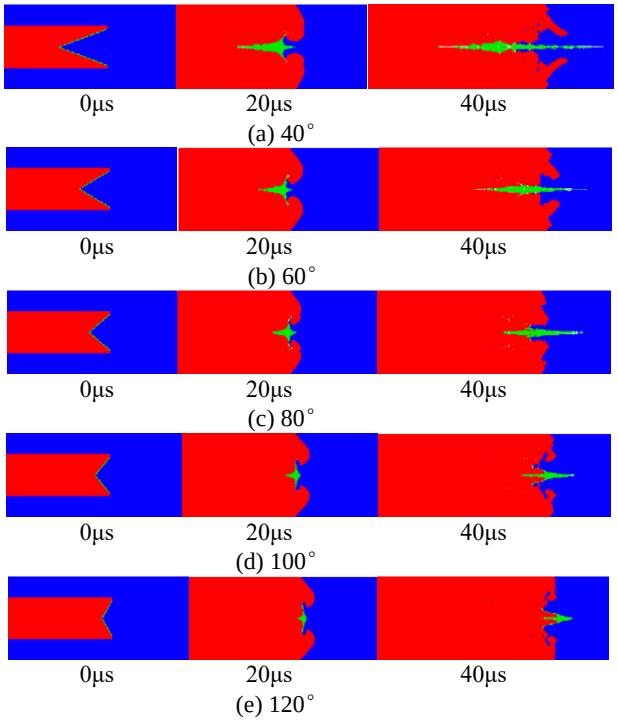

Fig.4. The jet forming process at different cone angles.

It can be seen from Fig. 4 that the shaped jet of ZrCuNiAlAg amorphous alloy has been basically formed at 40μs, and the morphology of the jet at different cone angles are shown in Fig. 5.

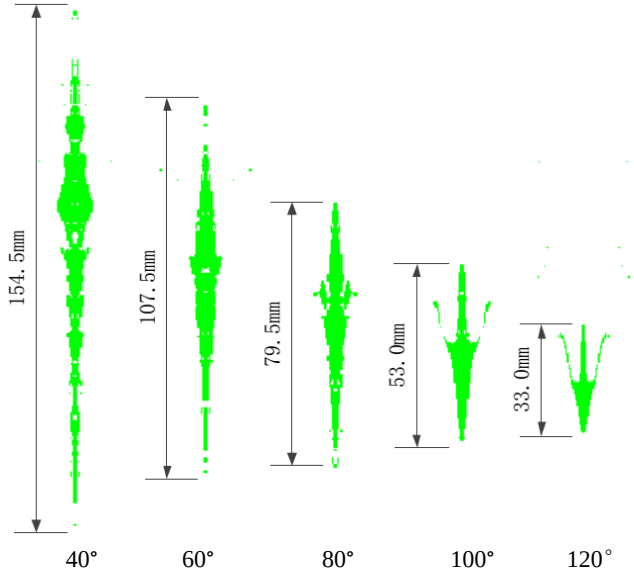

Fig.5. The jet morphology of the conical liner at different cone angles (40μs).

From Fig. 5, it can be seen that the jet becomes shorter and thicker from slender and long with the increase of the cone angle at 40μs, that is, the jet length diameter ratio (LDR) becomes smaller. The jet length at 120° (33.0mm) is 78.6% shorter than that at 40° (154.5mm). When the cone angle reaches 100 ° and 120 °, the jet has two obvious tail fins. The curves of the tip velocity and the LDR of the jet with different cone angles are shown in Fig. 6 and Fig. 7 respectively.

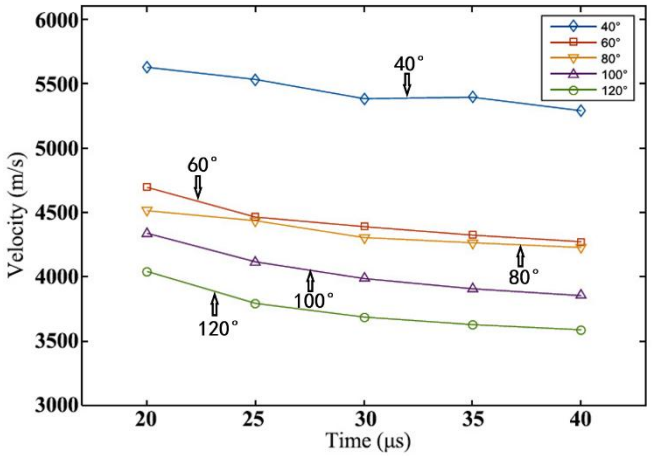

Fig.6. The jet tip velocity of different cone angles with time.

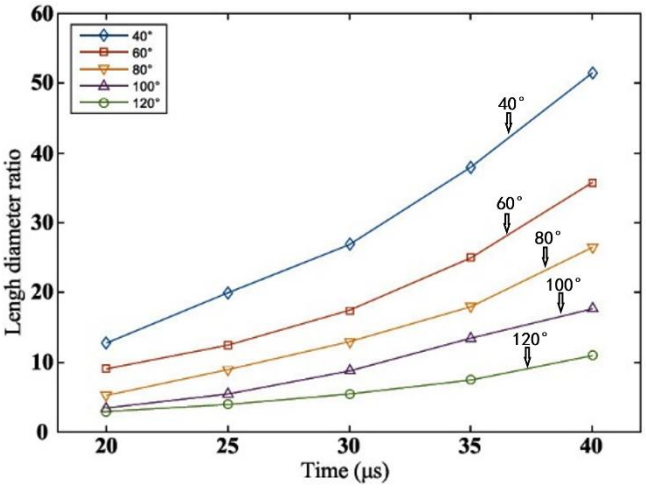

Fig.7. The jet LDR of different cone angles with time.

It can be seen from Fig. 6 and Fig. 7 that for the Zr-based amorphous alloy liner with a certain wall thickness (0.8mm), the tip velocity of the jet gradually decreases with time from collapsing to shaping of the liner, while the jet LDR gradually increases. Taking 60 ° cone angle as an example, the jet tip velocity (4384m/s) at 40μs is 6.72% lower than that at 20μs (4700m/s), and the jet LDR increases from 9.0 to 35.8, 2.98 times higher. The cone angle has an influence on both the tip velocity and the LDR of the jet. The smaller the cone angle is, the greater the jet tip velocity is. The jet tip velocity of 40° cone angle is significantly higher than that of the other four cone angles. Specifically, the tip velocity of 40° cone angle can reach 5290m/s at 40μs, which is 1.47 times of that of 120 ° cone angle liner at the same time. When the wall thickness is constant, the smaller the cone angle is, the larger the LDR is. The increasing trend of the jet LDR from the liner with a small cone angle is more obvious than that from the liner with a large cone

angle. The jet LDR of 40 ° cone angle liner is 4.68 times that of 120 ° cone angle liner at 40 μs. The jet parameters of different cone angles at 40μs are shown in the Table Ⅱ.

TABLE Ⅱ THE SHAPED JET PARAMETERS

Cone angle	Tip velocity (m/s)	length diameter ratio
40°	5290	51.5
60°	4384	35.8
80°	4229	26.5
100°	3856	17.7
120°	3591	11

B. Influence of wall thickness on jet forming performance

Keeping the SC structure unchanged, the cone angle of the liner is set to 60° . The jet forming process of ZrCuNiAlAg amorphous alloy is simulated when the wall thickness is 0.4mm, 1.2mm, 1.6mm, 2.0mm and 2.4mm respectively, as shown in Fig.8.

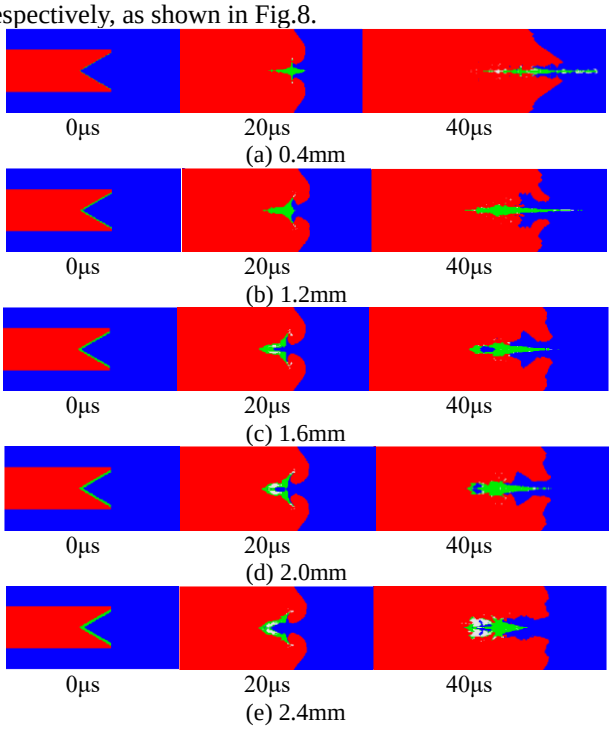

Fig.8. The jet forming process at different wall thicknesses.

At 40μs, the morphology of jet with different wall thickness are shown in Fig. 9.

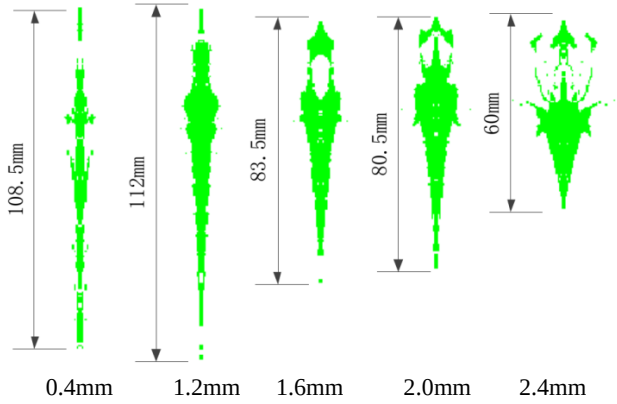

Fig.9. The jet morphology of the conical liner at different wall thickness (40μs).

It can be seen from Fig. 9 that the shaped jets formed by conical liners made of ZrCuNiAlAg amorphous alloy gradually change from slender to short and thick with the increase of wall thickness when they reach the same time. When the wall thickness is 2.4mm, the jet length (60mm) is 44.7% shorter than that when the wall thickness is 0.4mm (108.5mm). Compared with the jet tip, the shape of the slug also changes, gradually changing from solid to hollow and finally into divergent shape. The curves of the tip velocity and the LDR of the jet with different wall thicknesses are shown in Fig. 10 and Fig. 11 respectively.

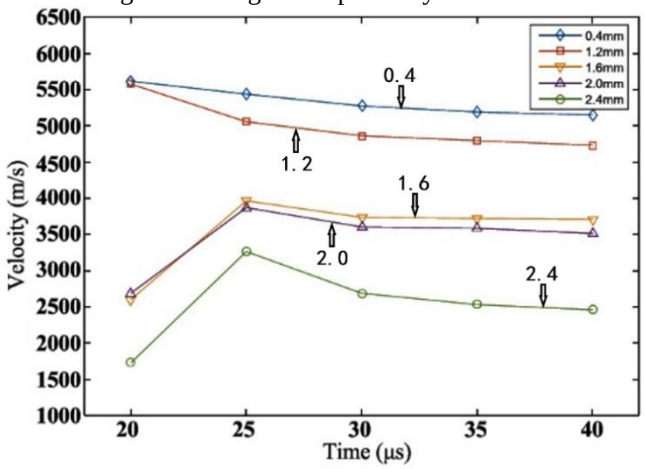

Fig.10. The jet tip velocity of different wall thicknesses with time.

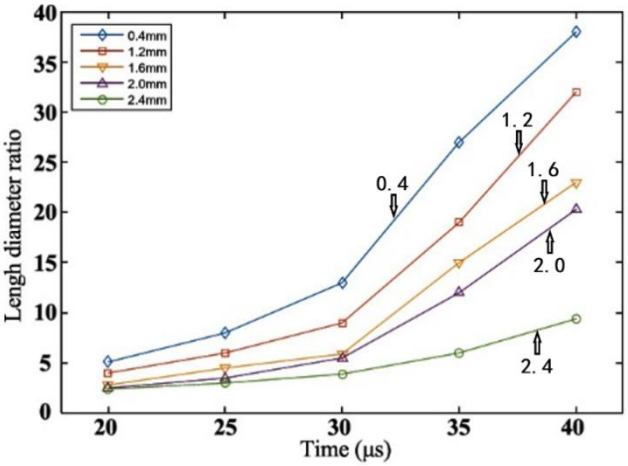

Fig.11. The jet LDR of different wall thicknesses with time.

Fig. 10 indicates that overall the smaller the wall thickness is, the greater the tip velocity of the jet is. The maximum tip velocity of the jet is about 5153m/s when the wall thickness is 0.4mm at 40μs, which is 2.09 times of the jet maximum tip velocity of the liner with wall thickness of 2.4mm at the same time. The tip velocity of the jet first increases and then decreases when the wall thickness is greater than 1.6mm. This is because with the increase of the wall thickness, the detonation energy consumed by crushing the liner during the jet forming is more than that when the wall thickness is smaller than 1.6mm. The time of jet forming increase significantly with the increasing wall thickness of the liner. The time for jet to reach its maximum velocity increase too. Fig. 11 indicates that the jet LDR increases with the decrease of the wall thickness of the liner. At 40 μs, the jet LDR formed by liner with wall thickness of 0.4mm is 4.13 times of that of 2.4mm liner. Taking the wall thickness of 1.2mm as an example, the jet LDR increases

from 4.0 at 20μs to 32.0 at 40μs, which is seven times larger. The jet LDR changes relatively slowly between 20μs and 30μs, but it increases significantly between 30μs and 40μs. The parameters of shaped jet with different wall thicknesses at 40μs are shown in Table III.

TABLE Ⅲ SHAPED JET PARAMETERS (CONE ANGLE=60°)

Wall thickness(mm)	Tip velocity(m/s)	LDR
0.4	5153	38
1.2	4734	32
1.6	3713	23
2.0	3517	20.3
2.4	2462	9.2

Ⅳ. PENETRATING EXPERIMENT OF ZrCuNiAlAg AMORPHOUS LINER

A. Test design

The SC structure for the static explosion test is shown in Fig. 12. The charge diameter (CD) is 45.8mm and the height of the SC is 98mm. The explosive consists of two parts: the front charge column and the rear charge column, both of which are all JH-2 explosive. The front charge column was stuck to the liner after been pressed. Point initiation mode is adopted and the SC is detonated by No.8 electric detonator. The material of the liner is ZrCuNiAlAg amorphous alloy. The liner has a conical shape with a cone angle of 40 ° and a wall thickness of 1.2mm. The experimental target is composed of several 45# steel plates with diameter of 100mm and thickness of 50mm or 20mm. According to the reference [16], the stand-off distance is set to 140 mm (about 3.0 CD).

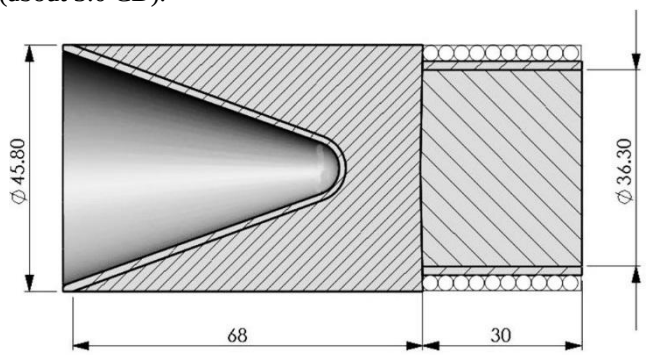

Fig.12. Structure of the SC.

The experiment conditions were checked in detail before the static explosion test to ensure safety. Then place several target blocks with appropriate thickness on the ground and a plastic support tube with a predetermined height on the top target block. Place the SC stably on the support tube and connect the detonating wire. Place the No. 8 electric detonator on the other end of the SC opposite to the liner and connect the electric detonator initiation device. Finally detonate the SC. The test process is shown in Fig. 13. Experiment results including penetration depth of the jet and the perforation entrance diameter are recorded after the test.

(a) Emplacing the warhead (b) Emplacing the detonator (c) Detonating the warhead

Fig.13. The process of static explosion experiment.

B. Results and analysis

a. Ground static explosion test results

Two rounds of static explosion tests of SC with ZrCuNiAlAg amorphous alloy liner were conducted. As shown in Table IV, the average penetration depth of the jet formed by the SC against the steel plate is 97.5mm, and the average penetration aperture is 25mm. The penetration damage effect against 45# steel target plate is shown in Fig. 14, where there is obvious "ablation" blackening phenomenon at the perforation entrance of steel target plate, which indicates that ZrCuNiAlAg amorphous alloy jet has a strong energy releasing effect during the process of penetrating the target plate.

TABLE Ⅳ STATIC EXPLOSION EXPERIMENT RESULTS OF SC

Serial number	Penetration depth （mm）	Perforation entrance diameter （mm）
1#	110	25
2#	85	25
Average value	97.5	25

Fig.14. Damage effect of penetration.

Fig.15 continuously recorded the penetration process and energy release of the energetic jet against 45# steel target plate. From the moment of initiation, the penetration and energy release process lasted about 791.67ms. The interval time between two adjacent frames is 41.67ms. Fig.15 (c) ~ (p) shows that obvious chemical reaction occurs during the penetration process against the steel plate of the jet formed by the Zr-based amorphous alloy liner. The corresponding reaction products and the debris eroded and peeled from the target plate fly out of the penetration tunnel along the opposite direction to the jet, thus it forms a sparks area with huge amount of high-speed and flaming sparks. The sparks area becomes from big to small, from truncated circular

cone to thin circular cone and the amount of the sparks in this area becomes less and less, the density of which becomes lower and finally gradually disappear. The aforementioned process can be described by the model in Fig.16. The perforation entrance turned over outwards after been scoured and eroded repeatedly during the process of a huge amount of sparks fly out of the penetration tunnel rapidly. And finally the perforation with a large diameter entrance is formed.

It can also be seen from Fig.15 that a strong deflagration reaction occurs at about 80ms after detonation. The dispersed range of deflagration and erosion products decreased significantly after 125ms. The deflagration intensity after 375ms was significantly reduced, and sparks were almost invisible after 625ms. It is almost certain that the deflagration reaction during the penetration has a negative effect on the penetration itself of the jet. Therefore, the penetration depth is obviously lower than that of the traditional inert copper jet under the same conditions.

b. Numerical simulation results

The AUTODYN numerical simulation model is established based on Fig. 12 for the SC structure. The liner material , the initiation mode, the initial and boundary conditions of the SC are the same as those in previous part of the paper. Simulation calculation is carried out for the process of the explosive detonation energy crushing the liner of SC to form the jet and the jet penetrating the steel target plate.

The numerical simulation process of jet forming is shown in Fig.17 (a). At 50μs, the jet just begins to contact the target plate. The jet at 50μs is extracted by the mapping method, and the 45# steel target plate model is established for simulating the penetration process of the jet into the 45# steel target plate, as shown in Fig. 17 (b). Simulation results show that the jet penetration depth into the steel target is 105mm, and the entrance diameter of the perforation is 22.8mm.

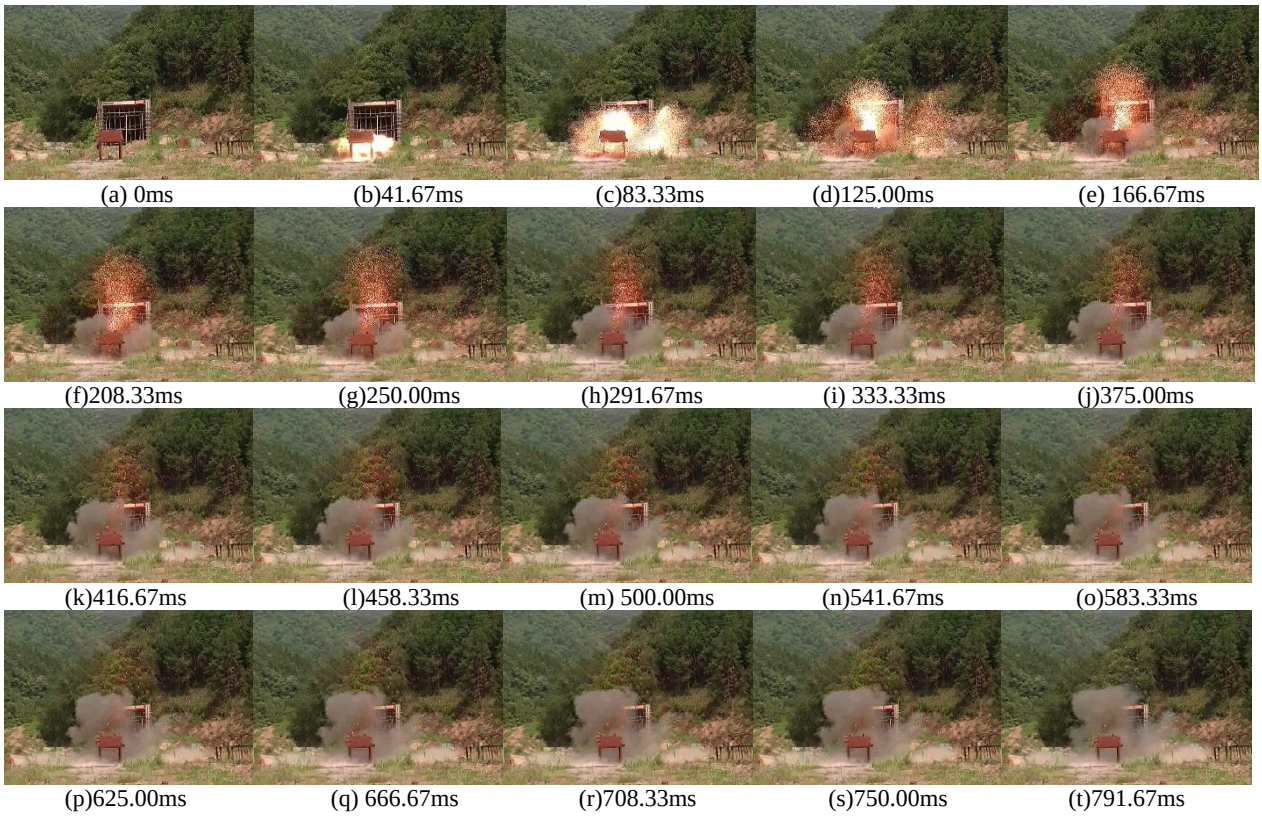

Fig. 15. The penetration and energy release process of the energetic jet.

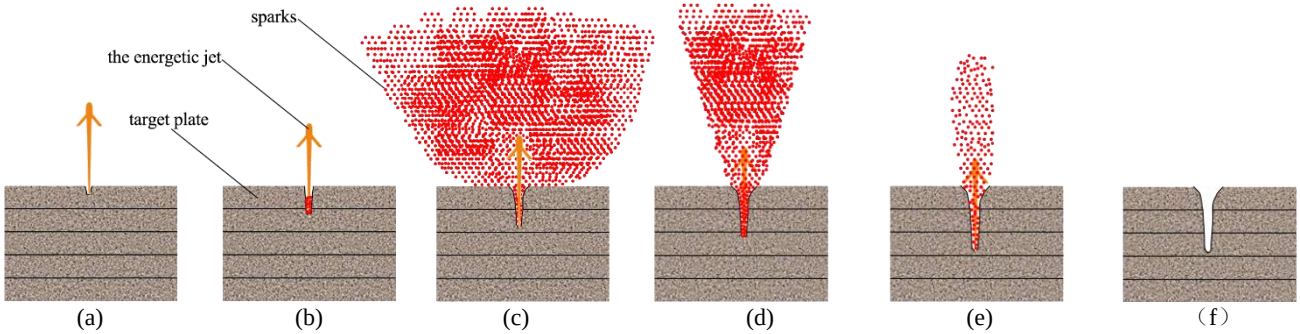

(a) Single penetration (b) Start stage of deflagration (c) Penetration and blast combined damage stage (d) Deflagration reaction weakens and penetration continues (e) Deflagration stops, the penetration depth no longer increases (f) End

Fig. 16. A simple model of penetration and blast combined damage process of the energetic jet.

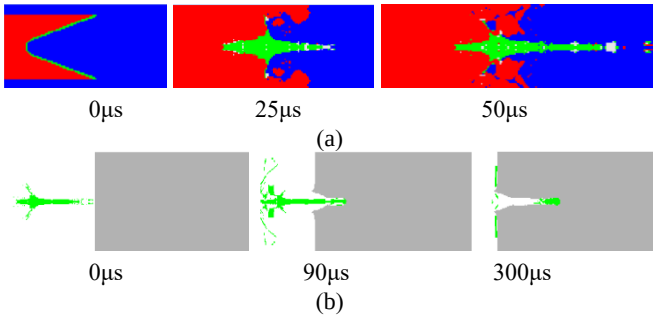

Fig.17. The jet forming and penetrating process.

c. Comparative analysis

Comparing the static explosion test and numerical simulation results of Zr-based amorphous alloy liner, it can be found that the penetration depth calculated by simulation is close to the static explosion test results of 1# SC, and it is better than the average value, with a deviation of 7.6%. The perforation diameter obtained by numerical simulation is smaller than that obtained by the static explosion test of SC, with a deviation of 8.8%, because the numerical simulation does not consider the energy-releasing characteristics and strong aftereffect of the jet from the Zr-based amorphous alloy liner during the penetrating against steel target. Compared with the static explosion test results, the deviation values of the penetration depth and perforation diameter obtained by numerical simulation are less than 10%, which shows that the modeling method, material parameter selection, initial condition and boundary condition setting adopted by numerical simulation in this paper are reasonable and feasible, and can well simulate the jet forming and penetration process of ZrCuNiAlAg amorphous alloy liner.

Ⅴ. CONCLUSION

（1）Under the action of explosive products, the conical ZrCuNiAlAg amorphous alloy liner can form a spindle shaped jet with good stability and continuity, which indicates that this kind of liner has good jet formability.

（2）The cone angle and wall thickness have a significant effect on the jet forming process of the conical ZrCuNiAlAg amorphous alloy SC. In a certain range, the tip velocity and length diameter ratio of the jet decrease with the increase of the cone angle of the liner. The jet gradually changes from slender shape to short thick shape with the increase of the wall thickness of the liner and the slug gradually changes from solid to hollow and finally becomes divergent. In a certain cone angle, the jet tip velocity and the length diameter ratio increase with the decrease of the wall thickness of the liner.

（3）For a conical ZrCuNiAlAg amorphous alloy liner with a cone angle of 40° and wall thickness of 1.2mm, the average penetration depth against 45# steel target plate is 97.5mm under the stand-off distance of 3 times of charge diameter, while the diameter of perforation entrance is 25mm. The deviation between the numerical simulation results and the static explosion test results is less than 10%.

（4）In the process of static explosion test, the active jet formed by Zr-based amorphous energetic alloy liner shows obvious energy-releasing characteristics, and has a significant aftereffect on the target plate. The penetration depth of reactive jet to the target plate is smaller than that of the inert jet, but the diameter of the perforation entrance increases obviously. The deflagration reaction and the deflagration products' reverse flight and strong erosion through the orifice are the main reasons for the formation of "large diameter, small penetration depth" perforation by energetic jet.

REFERENCES

[1] H. F. Wang, H. G. Guo, B. Q. Geng, Q. B. Yu, and Y. F. Zheng, “Application of PTFE/Al Reactive Materials for Double-Layered Liner SC,” *Materials*, vol. 12, no. 16, 2019,pp. 2768.

[2] F.Y. Xu, Y. F. Zheng, Q. B. Yu, Y. Z. Wang, and H. F. Wang, “Experimental Study on Penetration Behavior of Reactive Material Projectile Impacting Aluminum Plate,” *International Journal of Impact Engineering*, vol. 95, no. 9, 2016, pp. 125-132.

[3] Y. F. Zheng, C. H. Su, H. G. Guo, Q. B. Yu, and H. F. Wang, “Behind-target Rupturing Effects of Sandwich-like Plates by Reactive Liner SC Jet,” *Propellants, Explosives. Pyrotechnics*, vol. 44, no. 11, 2019, pp. 1400-1409.

[4] J. G. Xiao, X. P. Zhang, Y. Z. Wang, F. Y. Xu, and H. F. Wang. “Demolition Mechanism and Behavior of SC with Reactive Liner,” *Propellants, Explosives, Pyrotechnics*, vol. 41, no. 4, 2016, pp. 612-617.

[5] H. G. Guo, Y. F. Zheng, Q. B. Yu, C. Ge, and H. F. Wang, “Penetration Behavior of Reactive Liner SC Jet Impacting Thick Steel Plates,” *International Journal of Impact Engineering*, vol. 126, no. 4, 2019, pp. 76-84.

[6] J. K. Laszlo, P. W. William, “Investigation of a Bulk Metallic Glass as a SC Liner Material,” in *Proceedings of the 23rd International Symposium on Ballistics*, Tarragona, Spain, Apr. 2007, pp.269-274.

[7] P. W. William, J. K. Laszlo, and E. P. Justin, “Investigation of a Bulk Metallic Glass as a SC Liner Material,” US: Aberdeen Proving Ground, US Army Research Laboratory, ARL-TR-3864, Aug. 2006.

[8] J. L. Han, X. Chen, Z. H. Du, H. M. Fu, Y. D. Jing, T. Yuan, C. Cheng, C. X. Du, and L. Z. Xu, “Application of W/Zr amorphous alloy for SC liner,” *Materials Research Express*, vol. 6, no. 11, 2019, pp. 115209.

[9] J. L. Han, X. Chen, Z. H. Du, H. M. Fu, C. Cheng, L. Z. Xu, J. B. Wang, and C. X. Du, “Compressive Mechanical Properties of W-particle/Zr-based Amorphous Alloy Composites,” *Materials Research Express*, vol. 6, no. 8, 2019, pp. 085206.

[10] Manfred Held, “SC Optimization Against ERA Targets,” *Propellants, Explosives, Pyrotechnics*, vol. 30, no. 3, 2005, pp. 216-223.

[11] Z. G. Jiao, D. W. Kou, and N. Du, “Influence on Formed JPC and JET by Liner Angle,” *Equipment Manufacturing Technology*, vol. 43, no. 12, 2015, pp. 38-40.

[12] T. Elshenawy, Q. M. Li, “Breakup Time of Zirconium SC Jet,” *Propellants, Explosives, Pyrotechnics*, vol. 38, no. 5, 2013, pp. 703-708.

[13] S. V. Fedorov, “Numerical Simulation of the Formation of Shaped-charge Jets from Hemispherical Liners of Degressive Thickness,” *Combustion, Explosion, and Shock Waves*, vol. 52, no. 5, 2016, pp. 600-612.

[14] S. V. Fedorov, Ya. M. Bayanova, and S. V. Ladov, “Numerical Analysis of the Effect of the Geometric Parameters of a Combined Shaped-charge Liner on the Mass and Velocity of Explosively Formed Compact Elements,” *Combustion, Explosion, and Shock Waves*, vol. 51, no. 1, 2015, pp. 130-142.

[15] Y. X. Shi, D. M. Shi, W. Z. Li, Z. T. Yu, and C. M. Shang, “Study on JH-2 Model of the ZrCuNiAlAg Bulk Amorphous Alloy,” *Explosion and Shock Waves*, vol. 39, no. 9, 2019, pp. 093104-1-093104-8.

[16] P. Cui, D. S. Wang, D. M. Shi, J. Q. Xu, and J. W. Zhen, “Investigation of Penetration Performance of Zr-based Amorphous Alloy Liner Compared with Copper,” *Materials*, vol. 13, no. 4, 2020,pp. 912.